HHS Public Access

Author manuscript

Mol Genet Metab. Author manuscript; available in PMC 2024 February 01.

Published in final edited form as:

Mol Genet Metab. ; 138(2): 107371. doi:10.1016/j.ymgme.2023.107371.

Proteomics Identifies Novel Biomarkers of Synovial Joint Disease in a Canine Model of Mucopolysaccharidosis I

Chenghao Zhang[1], **Rahul Gawri**[1], **Yian Khai Lau**[1], **Lynn A. Spruce**[2], **Hossein Fazelinia**[2], **Zhirui Jiang**[1], **Stephanie Y. Jo**[3], **Carla R. Scanzello**[4,5], **Wilfried Mai**[6], **George R. Dodge**[1], **Margret L. Casal**[6], **Lachlan J. Smith**[1,8,+]

[1]Department of Orthopaedic Surgery, Perelman School of Medicine, University of Pe nnsylvania, 3450 Hamilton Walk, Philadelphia, PA, 19104 USA

[2]Proteomics Core Facility, Children's Hospital of Philadelphia, 3401 Civic Center Blvd, Philadelphia, PA 19104

[3]Department of Radiology, Perelman School of Medicine, University of Pennsylvania, 3400 Spruce Street, Philadelphia, PA 19104 USA

[4]Department of Medicine, Perelman School of Medicine, University of Pennsylvania, 3400 Spruce Street, Philadelphia, PA 19104 USA

[5]Department of Medicine, Corporal Michael J. Crescenz VA Medical Center, 3900 Woodland Ave, Philadelphia, PA 19104 USA

[6]Department of Clinical Sciences and Advanced Medicine, School of Veterinary Medicine, University of Pennsylvania, 3900 Spruce St, Philadelphia, PA 19104 USA

[8]Department of Neurosurgery, Perelman School of Medicine, University of Pennsylvania, 3400 Spruce Street, Philadelphia, PA 19104 USA

Abstract

Mucopolysaccharidosis I is a lysosomal storage disorder characterized by deficient alpha-L-iduronidase activity, leading to abnormal accumulation of glycosaminoglycans in cells and tissues.

[+]Correspondence : Lachlan J. Smith, Ph.D., Associate Professor, Department of Orthopaedic Surgery, Perelman School of Medicine, University of Pennsylvania, 371 Stemmler Hall, 3450 Hamilton Walk, Philadelphia, PA, 19104 USA, lachlans@pennmedicine.upenn.edu, Phone: +1 215 746 2169; Fax: +1 215 573 2133.

Author Contributions

CZ contributed to study design, performed experiments, interpreted findings and drafted the manuscript; LJS conceived the study, contributed to study design, interpreted findings and drafted the manuscript; RG and YKL contributed to study design, performed experiments and interpreted findings; MLC contributed to study design, performed physical examinations, interpreted findings and drafted the manuscript; GRD contributed to study design and interpretation of findings; WM contributed to development of the MRI grading scheme and interpretation of findings; and LAS, FH, ZJ, SYJ and CRS performed experiments. All authors provided critical feedback on the manuscript and approved the final version prior to submission.

Conflicts

LJS: Scientific Advisory Board, National MPS Society; Scientific Advisory Board, JOR Spine. GRD: Co-founder and CEO, Mechano-Therapeutics LLC. WM: Book royalties, "Diagnostic MRI in Dogs and Cats", Taylor and Francis. RG: Consultant, Acorn Biolabs; Scientific Advisory Board, JOR Spine. MLC, CRS, CZ, ZJ, YKL, SYJ, LAS, HF: No relevant disclosures.

Synovial joint disease is prevalent and significantly reduces patient quality of life. There is a critical need for improved understanding of joint disease pathophysiology in MPS I, including specific biomarkers to predict and monitor joint disease progression, and response to treatment. The objective of this study was to leverage the naturally-occurring MPS I canine model and undertake an unbiased proteomic screen to identify systemic biomarkers predictive of local joint disease in MPS I. Synovial fluid and serum samples were collected from MPS I and healthy dogs at 12 months-of-age, and protein abundance characterized using liquid chromatography tandem mass spectrometry. Stifle joints were evaluated postmortem using magnetic resonance imaging (MRI) and histology. Proteomics identified 40 proteins for which abundance was significantly correlated between serum and synovial fluid, including markers of inflammatory joint disease and lysosomal dysfunction. Elevated expression of three biomarker candidates, matrix metalloproteinase 19, inter-alpha-trypsin inhibitor heavy-chain 3 and alpha-1-microglobulin, was confirmed in MPS I cartilage, and serum abundance of these molecules was found to correlate with MRI and histological degenerative grades. The candidate biomarkers identified have the potential to improve patient care by facilitating minimally-invasive, specific assessment of joint disease progression and response to therapeutic intervention.

Keywords

Lysosomal storage disease; cartilage; inflammation; serum; synovial fluid; dog

Introduction

The mucopolysaccharidoses (MPS) are a family of inherited lysosomal storage disorders characterized by deficiencies in enzymes that degrade glycosaminoglycans (GAGs) [1]. These GAGs accumulate in cells and tissues resulting in progressive, multi-organ disease manifestations. There are 11 distinct types of MPS, each characterized by a unique enzyme deficiency resulting from a mutation in the associated gene [1]. The types of GAGs that accumulate also vary between MPS types, resulting in a spectrum of clinical manifestations. The incidence in the United States across all subtypes is estimated to be approximately 1 in 100,000 births [2]. While multiple organ systems are affected, skeletal manifestations are present in all MPS subtypes with varying degrees of severity [3]. Referred to collectively as dysostosis multiplex, these manifestations may include spinal deformity, short stature and synovial joint abnormalities [4–7]. Skeletal manifestations range from very mild to severe and in some cases require surgical correction [8, 9].

MPS I, also called Hurler Syndrome, or Hurler-Scheie or Scheie in its attenuated forms, is characterized by deficient α-L-iduronidase (IDUA) activity, leading to progressive accumulation of poorly degraded heparan and dermatan sulfate GAGs in multiple cell and tissue types [10]. Joint abnormalities in MPS I patients are prevalent, and patients experience significantly decreased quality of life due to pain and mobility impairment. Reported characteristics of joint disease include stiffness and limited range of motion, thought to result from abnormalities in the ligaments, joint capsules, and underlying epiphyseal bone [11, 12]. Almost all joints are involved, with the earliest presentation in shoulders, hands and knees [11, 12]. Patients report pain and difficulty completing daily activities, and

symptoms in undiagnosed patients may be mistaken for inflammatory rheumatic disorders [12]. Relatively little is known about the molecular pathophysiology of joint disease in MPS. Common characteristics across several disease subtypes, including MPS I, VI and VII, include inflammation-mediated articular cartilage destruction, impaired epiphyseal bone formation, and arthritic-like joint changes, all of which occur downstream of GAG accumulation [13–15].

Current clinical treatments for MPS I patients include enzyme replacement therapy (ERT) and hematopoietic stem cell transplantation; however, while these treatments effectively increase patient lifespan, they often fail to prevent progression of skeletal disease [16, 17]. Emerging therapeutic strategies such as gene therapy hold significant promise; however, sensitive and specific biomarkers for assessing the response of joint disease in clinical trials are lacking. Biomarkers are also essential for effective early diagnosis and monitoring of joint disease progression in MPS I patients. Application of gold standard radiological assessments, such as magnetic resonance imaging (MRI), is often challenging in MPS I patients due to their young age and cognitive impairment, and may necessitate potentially risky general anesthesia [18]. Protein biomarkers that can be measured systemically, for example in serum, plasma, urine or saliva, are a promising alternative. A handful of studies have used unbiased screening techniques to identify biomarkers of MPS more broadly, focusing on a limited number of subtypes [19–22]. There have also been more targeted studies that have sought to leverage the reported role of inflammation in MPS joint disease [13, 23]. For example, a recent study established correlations between inflammatory molecules present in plasma and urine, and degree of joint dysfunction in MPS patients [23]. To our knowledge, there have been no studies that have employed unbiased screening to identify molecular biomarkers specific for synovial joint disease in any MPS subtype. The naturally-occurring canine model of MPS I mimics the progressive synovial joint changes and decline in mobility that occur in human patients, and represents a powerful, clinically-relevant model for biomarker discovery and validation. The objective of this study was to leverage this model and undertake an unbiased proteomic screen to identify systemic molecular biomarker candidates predictive of local synovial joint disease in MPS I dogs.

Materials and Methods

Animals and Sample Collection

All animal work was conducted with approval from the University of Pennsylvania Institutional Animal Care and Use Committee. For this study, we used the naturally-occurring MPS I canine model. There were two study groups: MPS I-affected dogs (n=6; 3 males and 3 females) and healthy controls (n=5; 2 males and 3 females). MPS I dogs have a homozygous donor splice site mutation in intron 1 of the IDUA gene [24] and are considered to align most closely with the intermediate severity Hurler-Scheie phenotype found in human patients, based primarily on observed pathological manifestations in the central nervous system, skeleton and corneas [25, 26]. MPS I-affected animals were identified at birth by DNA mutation analysis. Control animals were heterozygous (phenotypically normal) littermates of MPS I dogs. Animals were raised and housed at the University of Pennsylvania School of Veterinary Medicine under NIH and USDA guidelines for the care

and use of animals in research. Animals were housed in kennel runs in groups of 2 or 3, with a light cycle of 12 hours per day and an ambient temperature of 21°C, with food and water provided ad libitum.

Physical examinations were performed monthly by a veterinarian (MLC), and included general clinical evaluations as well as specific assessments of mobility, gait, joint swelling and muscle tone. At 12 months-of-age, all animals were euthanized via an overdose of sodium pentobarbital consistent with the recommendations of the American Veterinary Medical Association. This terminal timepoint was selected as MPS I dogs typically manifest clear ambulatory deficits between 8 and 12 months-of-age. Prior to euthanasia, blood was collected from the cephalic vein, let sit for 30 min at room temperature until blood clots formed, then spun for 10 min in a refrigerated centrifuged at 3000 RCF for serum separation. Immediately following euthanasia, the right stifle (knee) joint was opened and synovial fluid (approximately 200 μl) was aspirated using an 18-gauge needle. Both serum and synovial fluid samples were then aliquoted, snap frozen in liquid nitrogen, and stored at −80°. The left stifle joint was collected, sealed in plastic and stored at −20°C for subsequent MRI and histological evaluation.

Proteomics

The detailed proteomics methodology is provided as supplementary information. Serum and synovial fluid samples were prepared for liquid chromatography tandem mass spectrometry (LC/MS/MS) analysis by solubilization, reduction, and alkylation followed by digestion with trypsin. The desalted samples were randomized and injected onto a Thermo QEHF mass spectrometer and collected using data independent acquisition. Spectronaut (version 15) [27] was employed for protein identification and quantification, using the reference Canus Lupus Familiaris proteome from Uniprot. Perseus (1.6.14.0) [28] was employed for data processing and statistical analysis using the MS2 intensity values generated by Spectronaut. The data were log2 transformed and normalized by subtracting the median for each sample. Statistical analysis of acquired data was performed as described below. The proteins that were exclusively detected in one experimental group were also reported for further bioinformatics analysis. Gene ontology (GO) and Kyoto Encyclopedia of Genes and Genomes (KEGG) pathway enrichment analyses were performed for both synovial fluid and serum results.

Magnetic Resonance Imaging

Left stifle joints were thawed at 4°C overnight and brought to room temperature, and imaged with musculature and skin intact using a 3T MR scanner (Magnetom Trio with TIM system; Siemens Healthcare, Malvern, PA, USA) and a 4-channel small flex coil, with the joint at an anatomical angle of 135° [29]. Three sequences were acquired: T2-weighted with fat suppression (TR/TE = 8050/77 ms); proton density-weighted (PD; TR/TE = 3900/40 ms); and T1-weighted volumetric interpolated breath-hold examination with water excitation (T1-VIBE; TR/TE = 10.4/4.9 ms). The slice thickness was 1.5 mm and field of view 140 mm for all sequences, and images were acquired in both the sagittal and dorsal (coronal) planes. For semi-quantitative assessment of joint pathology, a grading scheme was adapted using elements of both the Knee Osteoarthritis Scoring System (KOSS) and

MRI Osteoarthritis Knee Score (MOAKS) schemes [30, 31], inclusive of the following features: effusion synovitis (fluid effusions anterior/cranial to the joint), Baker's cysts (fluid effusions posterior/caudal to the joint), meniscal degeneration, meniscal extrusion, patellar displacement, fat pad synovitis, bone marrow edema, cartilage defects and subchondral cysts. Each feature was graded from 0 (absent) to 3 (severe) by three independent, blinded assessors. Overall grade was calculated as the sum of individual grades. Scores from individual reviewers were averaged prior to statistics.

Immunohistochemical Validation of Local Expression in Articular Cartilage

Following MRI, the distal femur was isolated from the left stifle joint, fixed in 10% neutral buffered formalin for 1 week and completely decalcified in formic acid/ethylenediaminetetraacetic acid (Formical 2000; Statlab, Louisville, USA). A 3 mm-thick mid-sagittal slice was then cut from the medial femoral condyle and processed into paraffin. Protein expression levels of three candidate biomarkers identified from the proteomic screen (matrix metalloproteinase 19 (MMP19), alpha-1-microglobulin (A1M) and inter-alpha-trypsin inhibitor heavy chain 3 (ITIH3)) in cartilage were examined using immunohistochemistry. Sections of healthy canine lung were used as a positive control for MMP19, while liver was used as a positive control for both A1M and ITIH3. Primary antibodies were purchased from Abcam (Cambridge, United Kingdom; catalog numbers ab53146, ab47980 and ab197188 for MMP19, A1M and ITIH3, respectively). Antigen retrieval was carried out on rehydrated sections using a heat mediated technique in a bath of Tris-EDTA pH 8.0 buffer for 15 minutes at 95°C. Sections were treated with 3% hydrogen peroxide followed by Background Buster (Innovex Biosciences; Richmond, USA), and then incubated with each primary antibody (1:200 for all) overnight at 4°C. Antibody staining was visualized using the Vectastain Elite ABC-Peroxidase Kit (Vector Laboratories; Burlingame, USA) and diaminobenzidine chromogen (Thermo Fisher Scientific; Waltham, USA). Finally, sections were counter stained with hematoxylin QS (Vector Laboratories) and cover-slipped with aqueous mounting medium (Agilent; Santa Clara, USA). For analysis, all slides were imaged under bright field light microscopy (Eclipse 90i; Nikon; Tokyo, Japan). For quantitative assessment of cell immunopositivity, three randomly selected regions of interest per section at 10X magnification and spanning the full cartilage thickness were analyzed. For each region, the number of immunopositive cells was counted and normalized as a percentage of the total number of cells present. Only cells with a nucleus were counted (i.e. empty lacunae were excluded). Cell counting for each region was performed by three individuals who were blinded to the study groups, averaged and taken as a single biological replicate for statistical comparisons.

Histological Grading of Articular Cartilage Condition

Histological sections 7 μm thick were double-stained with safranin O and fast green, and imaged under bright field light microscopy. Semi-quantitative grading of cartilage condition was performed using an adaptation of the OARSI guidelines for canine osteoarthritis by three independent and blinded assessors [32]. The following parameters were determined: cartilage structure (surface undulations/fissures), proteoglycan loss, and chondrocyte pathology (cell enlargement, increased cell numbers and/or increased cell clustering). Each section was divided into thirds across the width of the condyle, and

graded for local (1/3) multifocal (2/3) or global (3/3) pathology in each category, with scores ranging from 0 for completely healthy to 12 for severely degenerate [32]. Overall grade (sum of individual parameters) was also calculated. The scores from individual reviewers were averaged prior to statistics.

Statistical Analyses

For proteomics data, Perseus software was used to establish statistically-significant fold changes in protein abundance in MPS I vs control samples. Student's t-tests were employed to identify differentially abundant proteins using adjusted p values < 0.05 as the significance threshold. For proteins that were significantly different (MPS I vs control) for both serum and synovial fluid, correlations between the abundance (normalized log2 intensity) of each protein in serum and the same protein in synovial fluid were assessed using Pearson's tests. Normality of data distribution was confirmed using Shapiro-Wilk tests. Where data were normally distributed, significant differences in cartilage cell immunopositivity, histological grading parameters, and joint MRI grading parameters between control and MPS I were established using unpaired t-tests, and data presented as mean ± standard deviation. Where data were not normally distributed, Mann-Whitney tests were used, and data presented as median and interquartile range. Correlations between abundance (normalized log2 intensity) of selected biomarker candidates in both synovial fluid and serum, and overall cartilage and MRI grades were determined using Spearman's rank order tests. $P < 0.05$ was considered statistically significant for all tests.

Results

Clinical Findings

All animals reached the study end point of 12 months-of-age without any adverse events. Animals received comprehensive weekly physical examinations, which included clinical assessments of joint function and ambulatory ability. Throughout the duration of the study, no abnormalities were noted in control dogs. General clinical signs of disease in MPS I animals included corneal clouding that was mild progressing to moderate throughout the study, prominent third eyelids, erythematous conjunctivae, prognathism inferior, and thickened skin under the chin. All MPS I animals had reducible umbilical hernias, and 5 of 6 animals developed systolic heart murmurs between 5 and 8 months of age ranging in severity from I/VI to II/VI. With respect to skeletal disease manifestations, all MPS I animals were ambulatory throughout the study period; however, all had hyperextended carpi, stifles, and tarsi and widely splayed digits. Five of the 6 MPS I animals developed mild to moderate joint effusion between 2 and 7 months of age. The joints were neither painful nor warm to the touch.

Proteomics

For both synovial fluid and serum, principal component analyses (Figure 1A) demonstrated clustering of control and MPS I samples, confirming significant effects of disease state on relative protein abundance in both sample types. In synovial fluid, a total of 810 unique proteins were identified, of which 149 exhibited significantly different abundance in MPS I versus control (Figures 1B and C). Of these proteins, 101 were significantly upregulated

(Supplemental Table 1), and 48 were significantly downregulated (Supplemental Table 2). In serum, a total of 410 unique proteins were identified, of which 150 exhibited significantly different abundance in MPS I vs control (Figures 1B and C). Of these proteins, 85 were significantly upregulated (Supplemental Table 3), and 65 were significantly downregulated (Supplemental Table 4). The top 10 upregulated and down regulated proteins in both sample types are shown in Figures 2A–D. In synovial fluid, the top upregulated protein was transmembrane glycoprotein NMB (GPNMB, log2 fold change 6.32 in MPS I versus control, $p<0.001$). In serum the top upregulated protein was c-reactive protein (CRP, log2 fold change 2.89 in MPS I versus control, $p=0.003$). To identify candidate circulating biomarkers predictive of local synovial joint disease, we examined correlations between molecules with significantly differential abundance in both synovial fluid and serum. There were 50 proteins for which abundance was significantly different for both SF and serum, and of those, 40 exhibited a significant correlation in abundance (normalized log2 intensity) between synovial fluid and serum across all 11 samples (Table 1). Of these 40 candidate biomarkers, 19 were identified as being associated with inflammatory joint disease or lysosomal dysfunction based on an examination of prior literature (Figure 2E).

Pathway Analysis

For both synovial fluid and serum, the top GO terms (by number of molecules) were biological regulation, extracellular space and protein binding, for biological process, cellular component and molecular function, respectively (Figure 3A). Metabolic process was the second top biological process term for both sample types. With respect to KEGG analysis, the top enriched pathway for synovial fluid was innate immune system (Figure 3B). Other notable pathways amongst the top 10 included lysosome, and complement and coagulation cascade. For serum, the top enriched pathway was complement and coagulation cascade, while complement cascade and regulation of complement cascade were also among the top 10 pathways. The regulation of insulin-like growth factor (IGF) transport and uptake by insulin-like growth factor binding proteins (IGFBPs) pathway was also enriched for both sample types.

Immunohistochemical Validation of Local Expression in Articular Cartilage

Three candidate biomarkers identified through proteomic screening were selected for validation of local expression in stifle joint articular cartilage: matrix metalloproteinase 19 (MMP19), inter-alpha-trypsin inhibitor heavy chain 3 (ITIH3) and alpha-1-microglobulin (A1M). All three of these molecules exhibited significant upregulation in both synovial fluid and serum (Figure 2E), and significant correlation in abundance between synovial fluid and serum (Table 1). For ITIH3, the percentage of immunopositive cells was 2.5-fold higher in MPS I cartilage compared to control ($p=0.004$, Figure 4A). For MMP19, percentage of immunopositive cells was 2.6-fold higher in MPS I cartilage compared to control ($p=0.009$, Figure 4B). Finally, for A1M, the percentage of immunopositive cells was 2.0-fold higher in MPS I cartilage compared to control ($p=0.003$, Figure 4C).

Magnetic Resonance Imaging

Representative stifle joint MRI images (sagittal and dorsal) for control and MPS I animals are shown in Figures 5A and B. Elevated fluid cranial and caudal to the joint was frequently

observed in MPS I animals compared to controls. Meniscal intrasubstance degeneration and extrusion were occasionally observed, while articular cartilage structure appeared normal for most animals. Semi-quantitative grading (Figures 5C–L) revealed significantly worse effusion synovitis and overall MRI grade for MPS I animals compared to controls (p=0.015 and 0.024, respectively), while other individual grading parameters were not significantly different. In synovial fluid, A1M, ITIH3 and MMP19 abundance were all significantly and positively correlated with overall MRI grade (r=0.712, p=0.017; r=0.823, p=0.003; and r=0.777, p=0.007, respectively, Figures 5M–O), while CRP (the top upregulated molecule in serum) was not (r=0.400, p=0.222; Figure 5P). In serum, A1M and ITIH3 abundance were significantly and positively correlated with overall MRI grade (r=0.796, p=0.005; and r=0.713, p=0.017, respectively, Figures 5Q and R), while MMP19 and CRP were not (r=0.524, p=0.101; and r=0.574, p=0.085, respectively; Figures 5S and T).

Histological Grading of Articular Cartilage Condition

Representative images of safranin-O and fast green double-stained sections of articular cartilage from the medial femoral cartilage of control and MPS I animals are shown in Figures 6A and B. Qualitatively, MPS I cartilage appeared moderately degenerated, including generalized loss of proteoglycan staining, and cell clustering and enlargement, while the surface structure was generally intact. Semi-quantitative grading revealed that cartilage from MPS I animals exhibited significantly worse proteoglycan staining and overall grade (p=0.004 for both), compared to control cartilage, while chondrocyte pathology and cartilage structure were not significantly different (p=0.076 and p=0.992, respectively, Figures 6C–F). In synovial fluid, A1M, ITIH3 and MMP19 abundance were all significantly and positively correlated with overall cartilage grade (r=0.752, p=0.010; r=0.697, p=0.021; and r=0.825, p=0.003, respectively, Figures 6G–I), while CRP was not (r=0.424, p=0.195; Figure 6J). Similarly, in serum, A1M, ITIH3 and MMP19 abundance were significantly and positively correlated with overall cartilage grade (r=0.843, p=0.002; r=0.674, p=0.027; and r=0.820, p=0.003, respectively, Figures 6K–M), while CRP was not (r=0.542, p=0.089; Figure 6N).

Discussion

Many patients with MPS exhibit progressive and debilitating synovial joint disease that impairs their mobility and capacity for independent living. For reasons still not well understood, the severity of joint disease varies markedly both between and within MPS subtypes. Molecular biomarkers that detect early pathological changes in the joints of MPS patients would represent a powerful tool to be used in their clinical management, including assessing early response to therapeutic intervention. As MPS patients may be initially misdiagnosed as having other rheumatic disorders, such biomarkers may also serve as a first-line diagnostic assay. In this study, we leveraged a clinically relevant canine model in combination with unbiased proteomic screening to identify molecules that may serve as circulating biomarkers for joint disease in MPS I. By screening donor-matched synovial fluid and serum samples, we were able to identify a shortlist of 40 biomarker candidate molecules that exhibited high correlation between local and systemic abundance.

We confirmed tissue-level expression of three biomarker candidates, the abundance of which correlated positively with joint degenerative condition.

MRI and histological findings in this study implicate multiple component joint tissues in the etiology of joint disease in MPS I dogs, and the associated pathological changes share a number of similarities with more common arthritic diseases. For example, fluid effusions are commonly observed in the knees of osteoarthritis patients, are associated with inflammation of the synovium (synovitis), and often correlate with painful symptoms [33]. In articular cartilage, observed altered cellularity and diminished proteoglycan staining are also hallmarks of osteoarthritis, where they are associated with local inflammatory changes [34]. Similar findings were recently reported for MPS VII dog articular cartilage at 6 months-of-age [35]. Inflammation has been previously implicated in the etiology of MPS joint disease across several subtypes, including MPS I, in both human patients and animal models, and is due in part to activation of the innate immune system by accumulating GAG fragments that function as damage-associated molecular pathogens [13, 14, 23, 35–38]. Indeed, in the current study, pathway analysis identified the innate immune system as the top enriched pathway for MPS I synovial fluid. Previous studies in MPS I mice identified cartilage proteoglycan loss, elevated matrix metalloproteinase expression and abnormal morphology as characteristics of progressive joint disease [37, 39]. Clinically, elevated tumor necrosis factor alpha (TNF-α) was found to be associated with increased pain and disability in MPS patients [38]. Interleukin 1-beta (IL-1β) and TNF-α were found to be significantly elevated in MPS I patient plasma but not correlate with joint dysfunction, while interleukin-6 (IL-6), was found to exhibit a significant association with decreased joint range of motion over time [23].

In the current study, we identified a number of molecules upregulated in both MPS I synovial fluid and serum that have previously been explored as circulating biomarkers for more common arthritic diseases. The top upregulated molecule found in MPS I serum, c-reactive protein (CRP), is an acute phase protein secreted by hepatocytes, immune cells and other cell types that is used as a systemic marker of inflammation in rheumatoid arthritis patients, where serum levels have been shown to correlate with local, tissue-level inflammatory changes [40]. CRP as a biomarker of osteoarthritis is less-well established, but has been shown to be elevated and associated with pain and loss of physical function [41]. Chemerin (RARRES2) is a chemoattractant adipokine implicated in immune and metabolic homeostasis [42]. Serum chemerin levels are elevated in rheumatoid arthritis patients and correlate with joint swelling [43]. Chemerin is also elevated in the synovial fluid, synovium and articular cartilage of knee osteoarthritis patients, and correlates with disease severity [44–46]. Taken together, our findings suggest that MPS I joint disease pathophysiology shares common elements with both osteoarthritis and rheumatoid arthritis, and that repurposing drugs currently prescribed or under development for these diseases may be a promising strategy for treating MPS I joint disease. Notably, some inflammatory molecules identified in prior studies such as the cytokines IL-6, IL-1β and TNF-α were not found in our results. This likely reflects a limitation of our proteomics screen, which due to the high dynamic range, meant that molecules present in relatively low abundance may not have been detected, even though they may nonetheless be important disease mediators.

We also confirmed tissue-level expression in MPS I articular cartilage for three molecules, MMP19, ITIH3 and A1M, with less-well established roles in arthritic diseases. Serum and synovial fluid abundance of these molecules was found to significantly and positively correlate with overall joint and/or cartilage degenerative condition assessed using MRI and histology, respectively. MMP19 exhibited elevated local expression in MPS I cartilage, and while this enzyme has not been extensively studied in the context of joint disease, it is able to autoactivate and degrade important extracellular matrix components such as aggrecan and cartilage oligomeric matrix protein [47, 48]. MMP19 was previously found to be elevated in sera from patients with rheumatoid arthritis and systemic lupus erythematosus [49]. The inter-alpha-trypsin inhibitors (ITIs) have important roles in regulating inflammation and extracellular matrix stabilization, including binding hyaluronic acid [50]. ITI proteins are comprised of a light chain (bikunin, a chondroitin sulfate proteoglycan) and multiple heavy chains, such as ITIH3 [51]. There is evidence that the concentration of hyaluronic acid-bound ITIs is elevated in the synovial fluid from rheumatoid arthritis patients [52]. Interestingly, we found that ITIH3 expression was particularly pronounced in the superficial zone of MPS I cartilage, and it has been suggested that ITIs may have a role in the protection of the articular surface [53]. A1M is a member of the lipocalin protein family, and has a central role in the cleaning of oxidative waste products, macromolecular repair, and antioxidation protection [54]. Increased levels of A1M are present in the synovial fluid and serum of acute inflammatory arthritis patients [55], and there is evidence that increased oxidative stress in MPS contributes to disease progression in multiple tissues, including cartilage [56, 57].

The top upregulated molecule in synovial fluid was GPNMB (also called osteoactivin), a trans-membrane glycoprotein expressed by numerous cell types including chondrocytes [58, 59]. GPNMB is positive regulator of osteoblast differentiation [60] and also been linked to lysosomal dysfunction [36]. Elevated GPNMB expression has been linked to several lysosomal storage disorders, where it has been proposed as a potential biomarker [61–65]. Previously, we demonstrated elevated mRNA expression of GPNMB in the vertebral epiphyseal cartilage of very young MPS VII dogs [66]. In the current study, while GPNMB was upregulated in synovial fluid, similar upregulation was not found serum, suggesting it may not be a suitable systemic biomarker candidate for joint disease.

For biomarkers to serve as a first-line diagnostic tool in previously undiagnosed patients, they would need to be able to effectively distinguish between joint disease associated with MPS I versus other rheumatic disorders. Notably, several lysosome-related molecules including lysosome-associated membrane protein 2 (LAMP2), alpha-mannosidase (MAN2B1) and prosaposin (PSAP) were found to be upregulated in both MPS I synovial fluid and serum, and exhibited significant correlation between local and systemic expression. A panel of serum biomarkers that includes both markers of inflammatory joint disease and markers of lysosomal dysfunction could potentially represent a molecular signature unique to joint disease in MPS I.

In addition to the innate immune system, pathway analysis identified complement cascade-related pathways as enriched in MPS I in both synovial fluid and serum. The complement cascade is a first line of defense in innate immunity, and consists of more than 50

circulating and cell-associated proteins [67]. The complement system is important in the pathophysiology of osteoarthritis, and complement components are elevated in the synovial fluid of patients in the early stages of the disease [67]. Local activation of complement in osteoarthritic joints is thought to occur in part due to the release of extracellular matrix degradation components and cellular debris from cartilage and synovial membrane [67]. Complement activation is also implicated in the pathogenesis of joint disease in rheumatoid arthritis patients [68]. Previously, in MPS VII mice, complement activation was shown to contribute to the pathogenesis of aortic dilatation [69]. Here, we provide evidence that complement activation may contribute to the progression of synovial joint disease in MPS I. Drugs that inhibit complement components are approved for treating several autoimmune disorder [70], and may represent a possible strategy for treating inflammatory disease in MPS I.

Limitations of this study include the afore-mentioned high dynamic range of the proteomic screen that may have precluded detection of some low abundance molecules. Tissue level validation was only performed for a small number of molecules and only in articular cartilage. A relatively small cohort of animals was studied, precluding an analysis of sex-dependent effects, and the capacity of biomarkers to predict joint disease severity within the MPS I cohort alone. Future studies will expand validation studies to additional molecules and joint tissues, and establish the potential for biomarkers to predict functional as well as structural changes. In conclusion, in this study we leveraged the clinically relevant canine model and unbiased proteomic screening to identify a panel of novel candidate biomarkers for synovial joint disease in MPS I. These biomarkers have the potential to improve patient care by facilitating minimally-invasive, specific assessment of joint disease progression and response to therapeutic intervention.

Supplementary Material

Refer to Web version on PubMed Central for supplementary material.

Acknowledgments

Funding for this work was received from the Department of Orthopaedic Surgery at the University of Pennsylvania and the National Institutes of Health (R01AR071975, P40OD010939 and P30AR069619). Animal care provided by the staff of the Referral Center for Animal Models of Human Genetic Disease and technical assistance provided by the staff of the Large Animal Imaging Facility at the University of Pennsylvania is gratefully acknowledged.

Data Availability Statement

The mass spectrometry proteomics data have been deposited to the ProteomeXchange Consortium via the PRIDE partner repository [71] with the dataset identifier PXD037130. Additional study data may be provided upon reasonable request to the corresponding author.

References

[1]. Neufeld EF, Muenzer J, The Mucopolysaccharidoses, in: Scriver CR, Beaudet AL, Sly WS, Valle D (Eds.), The metabolic and molecular bases of inherited disease, McGraw-Hill, New York, 2001, pp. 3421–3452.

[2]. Puckett Y, Mallorga-Hernandez A, Montano AM, Epidemiology of mucopolysaccharidoses (MPS) in United States: challenges and opportunities Orphanet J Rare Dis 16 (2021) 241. [PubMed: 34051828]

[3]. White KK, Orthopaedic aspects of mucopolysaccharidoses Rheumatology 50 (2011) V26–V33. [PubMed: 22210667]

[4]. Palmucci S, Attina G, Lanza ML, Belfiore G, Cappello G, Foti PV, Milone P, Di Bella D, Barone R, Fiumara A, Sorge G, Ettorre GC, Imaging findings of mucopolysaccharidoses: a pictorial review Insights Imaging 4 (2013) 443–459. [PubMed: 23645566]

[5]. Muenzer J, The mucopolysaccharidoses: a heterogeneous group of disorders with variable pediatric presentations J Pediatr 144 (2004) S27–34. [PubMed: 15126981]

[6]. Morishita K, Petty RE, Musculoskeletal manifestations of mucopolysaccharidoses Rheumatology (Oxford) 50 Suppl 5 (2011) v19–25. [PubMed: 22210666]

[7]. Montano AM, Lock-Hock N, Steiner RD, Graham BH, Szlago M, Greenstein R, Pineda M, Gonzalez-Meneses A, Coker M, Bartholomew D, Sands MS, Wang R, Giugliani R, Macaya A, Pastores G, Ketko AK, Ezgu F, Tanaka A, Arash L, Beck M, Falk RE, Bhattacharya K, Franco J, White KK, Mitchell GA, Cimbalistiene L, Holtz M, Sly WS, Clinical course of sly syndrome (mucopolysaccharidosis type VII) J Med Genet 53 (2016) 403–418. [PubMed: 26908836]

[8]. van der Linden MH, Kruyt MC, Sakkers RJ, de Koning TJ, Oner FC, Castelein RM, Orthopaedic management of Hurler's disease after hematopoietic stem cell transplantation: a systematic review J Inherit Metab Dis 34 (2011) 657–669. [PubMed: 21416194]

[9]. Ashby E, Eastwood D, Characterization of knee alignment in children with mucopolysaccharidosis types I and II and outcome of treatment with guided growth J Child Orthop 9 (2015) 227–233. [PubMed: 26076735]

[10]. Hampe CS, Eisengart JB, Lund TC, Orchard PJ, Swietlicka M, Wesley J, McIvor RS, Mucopolysaccharidosis Type I: A Review of the Natural History and Molecular Pathology Cells 9 (2020).

[11]. Guffon N, Journeau P, Brassier A, Leger J, Chevallier B, Growth impairment and limited range of joint motion in children should raise suspicion of an attenuated form of mucopolysaccharidosis: expert opinion Eur J Pediatr 178 (2019) 593–603. [PubMed: 30740618]

[12]. Mitrovic S, Gouze H, Gossec L, Schaeyerbeke T, Fautrel B, Mucopolysaccharidoses seen in adults in rheumatology Joint Bone Spine 84 (2017) 663–670. [PubMed: 28196778]

[13]. Simonaro CM, D'Angelo M, Haskins ME, Schuchman EH, Joint and bone disease in mucopolysaccharidoses VI and VII: identification of new therapeutic targets and biomarkers using animal models Pediatr Res 57 (2005) 701–707. [PubMed: 15746260]

[14]. Simonaro CM, D'Angelo M, He X, Eliyahu E, Shtraizent N, Haskins ME, Schuchman EH, Mechanism of glycosaminoglycan-mediated bone and joint disease: implications for the mucopolysaccharidoses and other connective tissue diseases Am J Pathol 172 (2008) 112–122. [PubMed: 18079441]

[15]. Peck SH, O'Donnell PJ, Kang JL, Malhotra NR, Dodge GR, Pacifici M, Shore EM, Haskins ME, Smith LJ, Delayed hypertrophic differentiation of epiphyseal chondrocytes contributes to failed secondary ossification in mucopolysaccharidosis VII dogs Molecular Genetics & Metabolism 116 (2015) 195–203. [PubMed: 26422116]

[16]. Taylor C, Brady P, O'Meara A, Moore D, Dowling F, Fogarty E, Mobility in Hurler syndrome J Pediatr Orthop 28 (2008) 163–168. [PubMed: 18388709]

[17]. Langereis EJ, den Os MM, Breen C, Jones SA, Knaven OC, Mercer J, Miller WP, Kelly PM, Kennedy J, Ketterl TG, O'Meara A, Orchard PJ, Lund TC, van Rijn RR, Sakkers RJ, White KK, Wijburg FA, Progression of Hip Dysplasia in Mucopolysaccharidosis Type I Hurler After Successful Hematopoietic Stem Cell Transplantation J Bone Joint Surg Am 98 (2016) 386–395. [PubMed: 26935461]

[18]. Lao HC, Lin YC, Liang ML, Yang YW, Huang YH, Chan YL, Hsu YW, Lin SP, Chuang CK, Cheng JK, Lin HY, The Anesthetic Strategy for Patients with Mucopolysaccharidoses: A Retrospective Cohort Study J Pers Med 12 (2022).

[19]. Alvarez JV, Bravo SB, Chantada-Vazquez MP, Barbosa-Gouveia S, Colon C, Lopez-Suarez O, Tomatsu S, Otero-Espinar FJ, Couce ML, Plasma Proteomic Analysis in Morquio A Disease Int J Mol Sci 22 (2021).

[20]. Alvarez VJ, Bravo SB, Chantada-Vazquez MP, Colon C, De Castro MJ, Morales M, Vitoria I, Tomatsu S, Otero-Espinar FJ, Couce ML, Characterization of New Proteomic Biomarker Candidates in Mucopolysaccharidosis Type IVA Int J Mol Sci 22 (2020).

[21]. Heywood WE, Camuzeaux S, Doykov I, Patel N, Preece RL, Footitt E, Cleary M, Clayton P, Grunewald S, Abulhoul L, Chakrapani A, Sebire NJ, Hindmarsh P, de Koning TJ, Heales S, Burke D, Gissen P, Mills K, Proteomic Discovery and Development of a Multiplexed Targeted MRM-LC-MS/MS Assay for Urine Biomarkers of Extracellular Matrix Disruption in Mucopolysaccharidoses I, II, and VI Anal Chem 87 (2015) 12238–12244. [PubMed: 26537538]

[22]. Yuan X, Meng Y, Chen C, Liang S, Ma Y, Jiang W, Duan J, Wang C, Proteomic approaches in the discovery of potential urinary biomarkers of mucopolysaccharidosis type II Clin Chim Acta 499 (2019) 34–40. [PubMed: 31469979]

[23]. Lund TC, Doherty TM, Eisengart JB, Freese RL, Rudser KD, Fung EB, Miller BS, White KK, Orchard PJ, Whitley CB, Polgreen LE, Biomarkers for prediction of skeletal disease progression in mucopolysaccharidosis type I JIMD Rep 58 (2021) 89–99. [PubMed: 33728251]

[24]. Menon KP, Tieu PT, Neufeld EF, Architecture of the canine IDUA gene and mutation underlying canine mucopolysaccharidosis I Genomics 14 (1992) 763–768. [PubMed: 1339393]

[25]. Shull RM, Helman RG, Spellacy E, Constantopoulos G, Munger RJ, Neufeld EF, Morphologic and biochemical studies of canine mucopolysaccharidosis I The American journal of pathology 114 (1984) 487–495. [PubMed: 6320652]

[26]. Spellacy E, Shull RM, Constantopoulos G, Neufeld EF, A canine model of human alpha-L-iduronidase deficiency Proc Natl Acad Sci U S A 80 (1983) 6091–6095. [PubMed: 6412235]

[27]. Bruderer R, Bernhardt OM, Gandhi T, Miladinovic SM, Cheng LY, Messner S, Ehrenberger T, Zanotelli V, Butscheid Y, Escher C, Vitek O, Rinner O, Reiter L, Extending the limits of quantitative proteome profiling with data-independent acquisition and application to acetaminophen-treated three-dimensional liver microtissues Mol Cell Proteomics 14 (2015) 1400–1410. [PubMed: 25724911]

[28]. Tyanova S, Temu T, Sinitcyn P, Carlson A, Hein MY, Geiger T, Mann M, Cox J, The Perseus computational platform for comprehensive analysis of (prote)omics data Nat Methods 13 (2016) 731–740. [PubMed: 27348712]

[29]. Galindo-Zamora V, Dziallas P, Ludwig DC, Nolte I, Wefstaedt P, Diagnostic accuracy of a short-duration 3 Tesla magnetic resonance protocol for diagnosing stifle joint lesions in dogs with non-traumatic cranial cruciate ligament rupture BMC Vet Res 9 (2013) 40. [PubMed: 23448526]

[30]. Kornaat PR, Ceulemans RY, Kroon HM, Riyazi N, Kloppenburg M, Carter WO, Woodworth TG, Bloem JL, MRI assessment of knee osteoarthritis: Knee Osteoarthritis Scoring System (KOSS)--inter-observer and intra-observer reproducibility of a compartment-based scoring system Skeletal Radiol 34 (2005) 95–102. [PubMed: 15480649]

[31]. Hunter DJ, Guermazi A, Lo GH, Grainger AJ, Conaghan PG, Boudreau RM, Roemer FW, Evolution of semi-quantitative whole joint assessment of knee OA: MOAKS (MRI Osteoarthritis Knee Score) Osteoarthritis and cartilage 19 (2011) 990–1002. [PubMed: 21645627]

[32]. Cook JL, Kuroki K, Visco D, Pelletier JP, Schulz L, Lafeber FP, The OARSI histopathology initiative - recommendations for histological assessments of osteoarthritis in the dog Osteoarthritis Cartilage 18 Suppl 3 (2010) S66–79. [PubMed: 20864024]

[33]. Hill CL, Gale DG, Chaisson CE, Skinner K, Kazis L, Gale ME, Felson DT, Knee effusions, popliteal cysts, and synovial thickening: association with knee pain in osteoarthritis J Rheumatol 28 (2001) 1330–1337. [PubMed: 11409127]

[34]. Fujii Y, Liu L, Yagasaki L, Inotsume M, Chiba T, Asahara H, Cartilage Homeostasis and Osteoarthritis Int J Mol Sci 23 (2022).

[35]. Gawri R, Lau YK, Lin G, Shetye SS, Zhang C, Jiang Z, Abdoun K, Scanzello CR, Jo SY, Mai W, Dodge GR, Casal ML, Smith LJ, Dose-Dependent Effects of Enzyme Replacement Therapy on

Skeletal Disease Progression in Mucopolysaccharidosis VII Dogs Molecular Therapy - Methods and Clinical Development In press (2022).

[36]. Simonaro CM, Ge Y, Eliyahu E, He X, Jepsen KJ, Schuchman EH, Involvement of the Toll-like receptor 4 pathway and use of TNF-alpha antagonists for treatment of the mucopolysaccharidoses Proc Natl Acad Sci U S A 107 (2010) 222–227. [PubMed: 20018674]

[37]. de Oliveira PG, Baldo G, Mayer FQ, Martinelli B, Meurer L, Giugliani R, Matte U, Xavier RM, Characterization of joint disease in mucopolysaccharidosis type I mice Int J Exp Pathol 94 (2013) 305–311. [PubMed: 23786352]

[38]. Polgreen LE, Vehe RK, Rudser K, Kunin-Batson A, Utz JJ, Dickson P, Shapiro E, Whitley CB, Elevated TNF-alpha is associated with pain and physical disability in mucopolysaccharidosis types I, II, and VI Mol Genet Metab 117 (2016) 427–430. [PubMed: 26873528]

[39]. Ferreira NY, do Nascimento CC, Pereira VG, de Oliveira F, Medalha CC, da Silva VC, D'Almeida V, Biomechanical and histological characterization of MPS I mice femurs Acta Histochem 123 (2021) 151678. [PubMed: 33434858]

[40]. Pope JE, Choy EH, C-reactive protein and implications in rheumatoid arthritis and associated comorbidities Semin Arthritis Rheum 51 (2021) 219–229. [PubMed: 33385862]

[41]. Jin X, Beguerie JR, Zhang W, Blizzard L, Otahal P, Jones G, Ding C, Circulating C reactive protein in osteoarthritis: a systematic review and meta-analysis Ann Rheum Dis 74 (2015) 703–710. [PubMed: 24363360]

[42]. Gomez R, Conde J, Scotece M, Gomez-Reino JJ, Lago F, Gualillo O, What's new in our understanding of the role of adipokines in rheumatic diseases? Nat Rev Rheumatol 7 (2011) 528–536. [PubMed: 21808287]

[43]. Gonzalez-Ponce F, Gamez-Nava JI, Perez-Guerrero EE, Saldana-Cruz AM, Vazquez-Villegas ML, Ponce-Guarneros JM, Huerta M, Trujillo X, Contreras-Haro B, Rocha-Munoz AD, Carrillo-Escalante MO, Sanchez-Rodriguez EN, Gomez-Ramirez EE, Nava-Valdivia CA, Cardona-Munoz EG, Gonzalez-Lopez L, D. Research Group for the Assessment of Prognosis Biomarkers in Autoimmune, Serum chemerin levels: A potential biomarker of joint inflammation in women with rheumatoid arthritis PLoS One 16 (2021) e0255854. [PubMed: 34506500]

[44]. Huang K, Du G, Li L, Liang H, Zhang B, Association of chemerin levels in synovial fluid with the severity of knee osteoarthritis Biomarkers 17 (2012) 16–20. [PubMed: 22080616]

[45]. Timur UT, Jahr H, Anderson J, Green DC, Emans PJ, Smagul A, van Rhijn LW, Peffers MJ, Welting TJM, Identification of tissue-dependent proteins in knee OA synovial fluid Osteoarthritis Cartilage 29 (2021) 124–133.

[46]. Biskup JJ, Balogh DG, Haynes KH, Freeman AL, Conzemius MG, Mechanical strength of four allograft fixation techniques for ruptured cranial cruciate ligament repair in dogs Am J Vet Res 76 (2015) 411–419. [PubMed: 25909373]

[47]. Stracke JO, Fosang AJ, Last K, Mercuri FA, Pendas AM, Llano E, Perris R, Di Cesare PE, Murphy G, Knauper V, Matrix metalloproteinases 19 and 20 cleave aggrecan and cartilage oligomeric matrix protein (COMP) FEBS Lett 478 (2000) 52–56. [PubMed: 10922468]

[48]. Stracke JO, Hutton M, Stewart M, Pendas AM, Smith B, Lopez-Otin C, Murphy G, Knauper V, Biochemical characterization of the catalytic domain of human matrix metalloproteinase 19. Evidence for a role as a potent basement membrane degrading enzyme J Biol Chem 275 (2000) 14809–14816. [PubMed: 10809722]

[49]. Sedlacek R, Mauch S, Kolb B, Schatzlein C, Eibel H, Peter HH, Schmitt J, Krawinkel U, Matrix metalloproteinase MMP-19 (RASI-1) is expressed on the surface of activated peripheral blood mononuclear cells and is detected as an autoantigen in rheumatoid arthritis Immunobiology 198 (1998) 408–423. [PubMed: 9562866]

[50]. Bost F, Diarra-Mehrpour M, Martin JP, Inter-alpha-trypsin inhibitor proteoglycan family--a group of proteins binding and stabilizing the extracellular matrix Eur J Biochem 252 (1998) 339–346. [PubMed: 9546647]

[51]. Zhuo L, Kimata K, Structure and function of inter-alpha-trypsin inhibitor heavy chains Connect Tissue Res 49 (2008) 311–320. [PubMed: 18991084]

[52]. Sandson J, Hamerman D, Schwick G, Altered properties of pathological hyaluronate due to a bound inter-alpha trypsin inhibitor Trans Assoc Am Physicians 78 (1965) 304–313. [PubMed: 4955886]

[53]. Smith SM, Melrose J, A Retrospective Analysis of the Cartilage Kunitz Protease Inhibitory Proteins Identifies These as Members of the Inter-alpha-Trypsin Inhibitor Superfamily with Potential Roles in the Protection of the Articulatory Surface Int J Mol Sci 20 (2019).

[54]. Akerstrom B, Gram M, A1M, an extravascular tissue cleaning and housekeeping protein Free Radic Biol Med 74 (2014) 274–282. [PubMed: 25035076]

[55]. Larsson S, Akerstrom B, Gram M, Lohmander LS, Struglics A, alpha1-Microglobulin Protects Against Bleeding-Induced Oxidative Damage in Knee Arthropathies Front Physiol 9 (2018) 1596. [PubMed: 30505280]

[56]. Pierzynowska K, Gaffke L, Cyske Z, Wegrzyn G, Buttari B, Profumo E, Saso L, Oxidative Stress in Mucopolysaccharidoses: Pharmacological Implications Molecules 26 (2021).

[57]. Simonaro CM, Haskins ME, Schuchman EH, Articular chondrocytes from animals with a dermatan sulfate storage disease undergo a high rate of apoptosis and release nitric oxide and inflammatory cytokines: a possible mechanism underlying degenerative joint disease in the mucopolysaccharidoses Lab Invest 81 (2001) 1319–1328. [PubMed: 11555679]

[58]. Karlsson C, Dehne T, Lindahl A, Brittberg M, Pruss A, Sittinger M, Ringe J, Genome-wide expression profiling reveals new candidate genes associated with osteoarthritis Osteoarthr Cartilage 18 (2010) 581–592.

[59]. Singh M, Del Carpio-Cano F, Belcher JY, Crawford K, Frara N, Owen TA, Popoff SN, Safadi FF, Functional Roles of Osteoactivin in Normal and Disease Processes Crit Rev Eukar Gene 20 (2010) 341–357.

[60]. Frara N, Abdelmagid SM, Sondag GR, Moussa FM, Yingling VR, Owen TA, Popoff SN, Barbe MF, Safadi FF, Transgenic Expression of Osteoactivin/gpnmb Enhances Bone Formation In Vivo and Osteoprogenitor Differentiation Ex Vivo J Cell Physiol 231 (2016) 72–83. [PubMed: 25899717]

[61]. Baldo G, Wu SS, Howe RA, Ramamoothy M, Knutsen RH, Fang JL, Mecham RP, Liu YL, Wu XB, Atkinson JP, Ponder KP, Pathogenesis of aortic dilatation in mucopolysaccharidosis VII mice may involve complement activation Molecular Genetics and Metabolism 104 (2011) 608–619. [PubMed: 21944884]

[62]. Parente MK, Rozen R, Cearley CN, Wolfe JH, Dysregulation of Gene Expression in a Lysosomal Storage Disease Varies between Brain Regions Implicating Unexpected Mechanisms of Neuropathology Plos One 7 (2012).

[63]. Kramer G, Wegdam W, Donker-Koopman W, Ottenhoff R, Gaspar P, Verhoek M, Nelson J, Gabriel T, Kallemeijn W, Boot RG, Laman JD, Vissers JPC, Cox T, Pavlova E, Moran MT, Aerts JM, van Eijk M, Elevation of glycoprotein nonmetastatic melanoma protein B in type 1 Gaucher disease patients and mouse models Febs Open Bio 6 (2016) 902–913.

[64]. Murugesan V, Liu J, Yang RH, Lin HQ, Lischuk A, Pastores G, Zhang XK, Chuang WL, Mistry PK, Validating glycoprotein non-metastatic melanoma B (gpNMB, osteoactivin), a new biomarker of Gaucher disease Blood Cell Mol Dis 68 (2018) 47–53.

[65]. Zigdon H, Savidor A, Levin Y, Meshcheriakova A, Schiffmann R, Futerman AH, Identification of a Biomarker in Cerebrospinal Fluid for Neuronopathic Forms of Gaucher Disease Plos One 10 (2015).

[66]. Peck SH, Tobias JW, Shore EM, Malhotra NR, Haskins ME, Casal ML, Smith LJ, Molecular profiling of failed endochondral ossification in mucopolysaccharidosis VII Bone 128 (2019) 115042. [PubMed: 31442675]

[67]. Schafer N, Grassel S, Involvement of complement peptides C3a and C5a in osteoarthritis pathology Peptides 154 (2022) 170815. [PubMed: 35598724]

[68]. Holers VM, Banda NK, Complement in the Initiation and Evolution of Rheumatoid Arthritis Front Immunol 9 (2018) 1057. [PubMed: 29892280]

[69]. Baldo G, Wu S, Howe RA, Ramamoothy M, Knutsen RH, Fang J, Mecham RP, Liu Y, Wu X, Atkinson JP, Ponder KP, Pathogenesis of aortic dilatation in mucopolysaccharidosis VII mice may involve complement activation Mol Genet Metab 104 (2011) 608–619. [PubMed: 21944884]

[70]. Galindo-Izquierdo M, Pablos Alvarez JL, Complement as a Therapeutic Target in Systemic Autoimmune Diseases Cells 10 (2021).

[71]. Perez-Riverol Y, Bai J, Bandla C, Garcia-Seisdedos D, Hewapathirana S, Kamatchinathan S, Kundu DJ, Prakash A, Frericks-Zipper A, Eisenacher M, Walzer M, Wang S, Brazma A, Vizcaino JA, The PRIDE database resources in 2022: a hub for mass spectrometry-based proteomics evidences Nucleic Acids Res 50 (2022) D543–D552. [PubMed: 34723319]

Highlights

- We identified 40 candidate serum biomarkers of joint disease in MPS I dogs.
- Biomarkers correlated with joint condition assessed using MRI and histology.
- Complement cascade-related pathways were implicated in joint disease etiology.
- Biomarkers may enable minimally-invasive assessment of joint disease in patients.

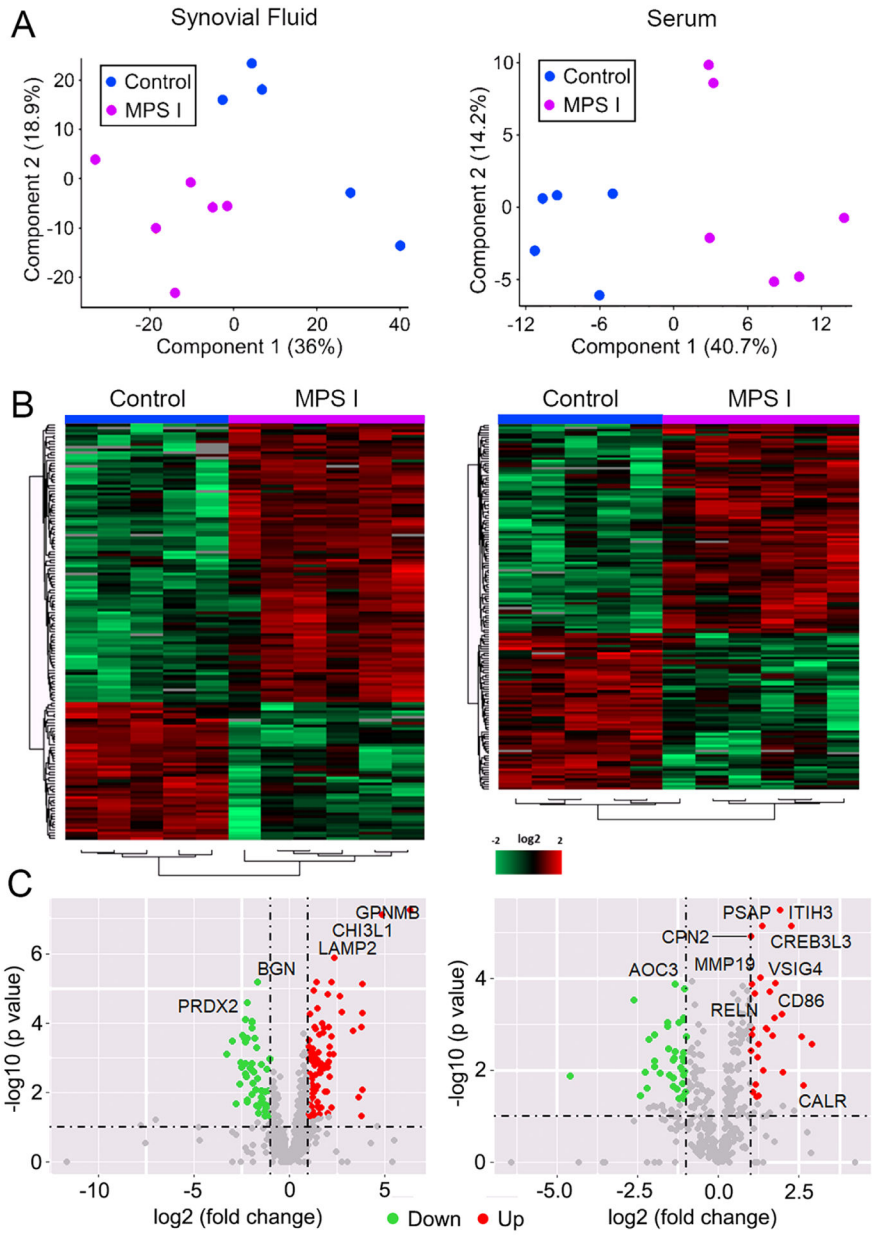

Figure 1.

Global analysis of proteomic screening of synovial fluid and serum from 12-month-old MPS I (n=6) and healthy control (n=5) dogs. **A.** Principal component analyses; **B.** Heat maps; and **C.** Volcano plots, showing clustering of samples, and relative up and down regulation of proteins as a function of disease state.

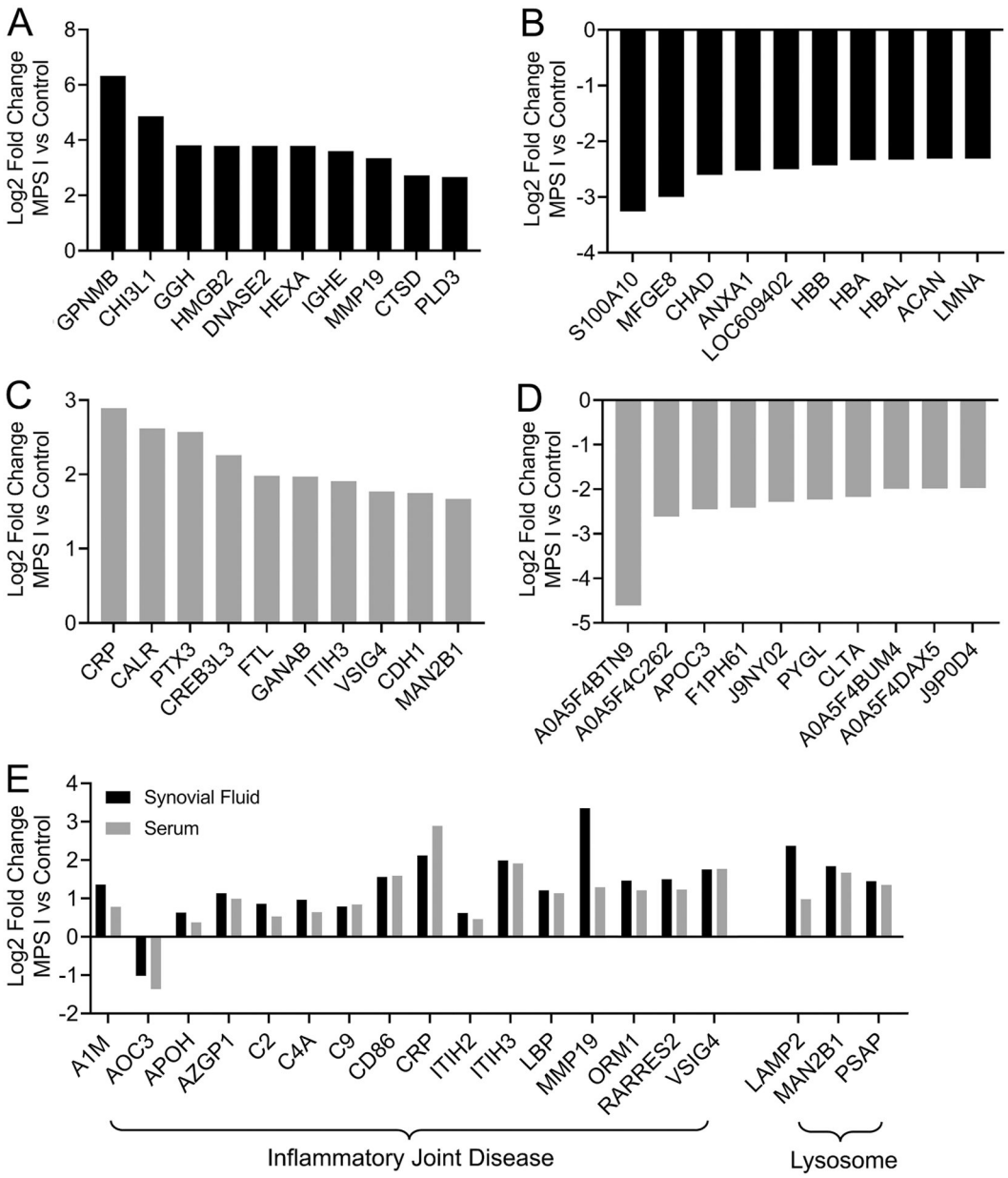

Figure 2.

Up and down regulation of selected proteins with significantly different abundance in MPS I dogs compared to controls. **A.** Top 10 proteins significantly upregulated and **B.** Downregulated in MPS I synovial fluid. **C.** Top 10 proteins significantly upregulated and **D.** Downregulated in MPS I serum. **E.** Selected proteins significantly up or down regulated in both MPS I synovial fluid and serum with previously described roles in inflammatory joint disease or lysosomal dysfunction. All $p<0.05$, N = 5–6.

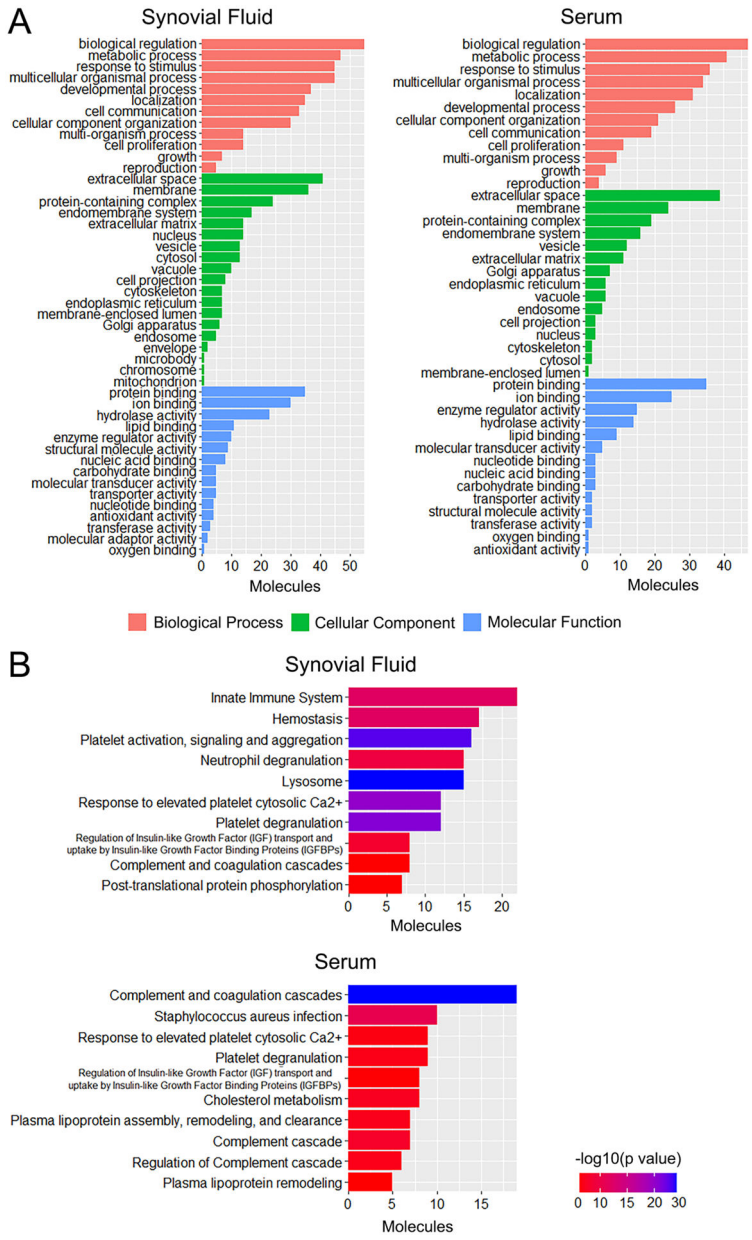

Figure 3.

Pathway analysis of proteomic screening results for synovial fluid and serum from 12-month-old MPS I (n=6) and healthy control (n=5) dogs. **A.** Gene ontology (GO) analysis. **B.** Kyoto Encyclopedia of Genes and Genomes (KEGG) pathway enrichment analysis.

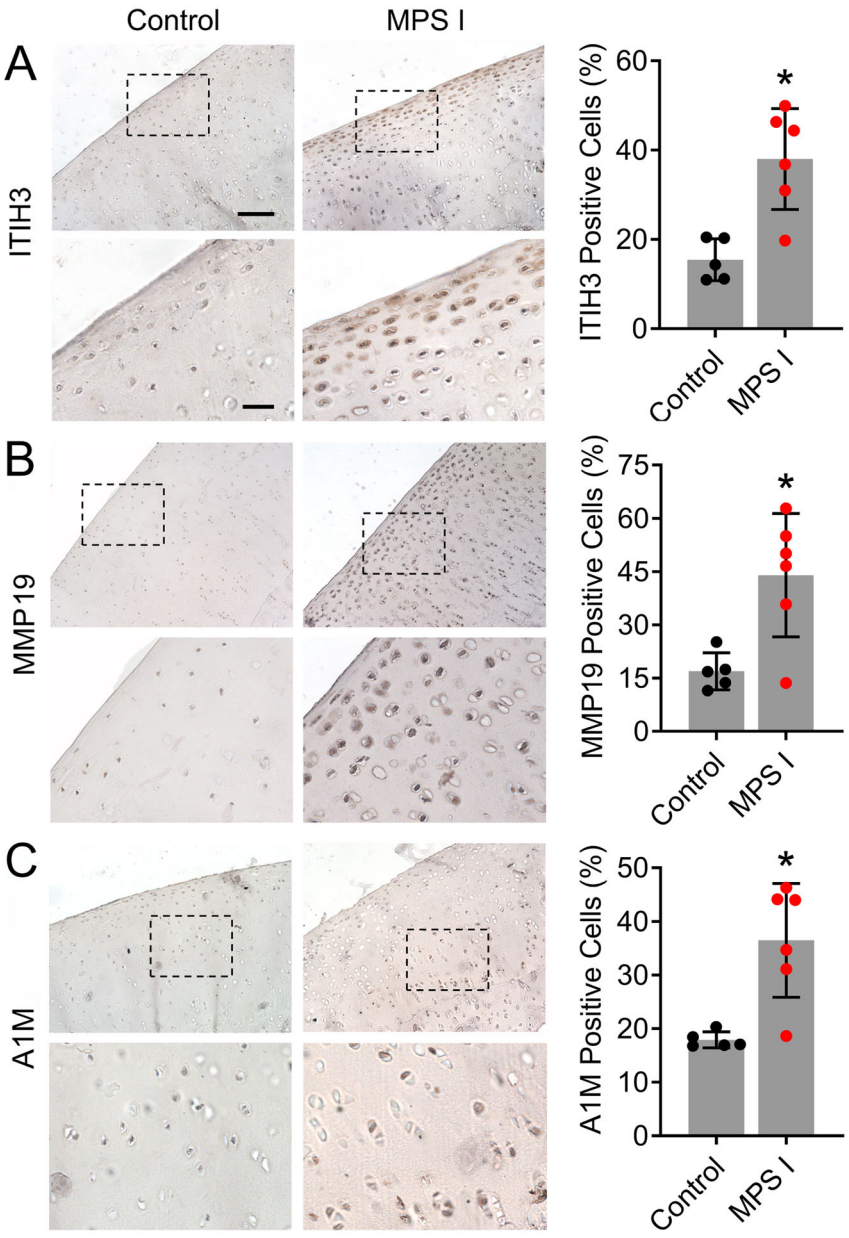

Figure 4.

Representative immunostaining and quantification of cells immunopositive for **A.** ITIH3; **B.** MMP19; and **C.** A1M in the femoral condylar cartilage of control and MPS I animals at 12 months-of-age. Scale = 100μm (higher magnification = 30μm); *p<0.05 vs control; N=5–6; mean ± SD; unpaired t-test; N = 5–6.

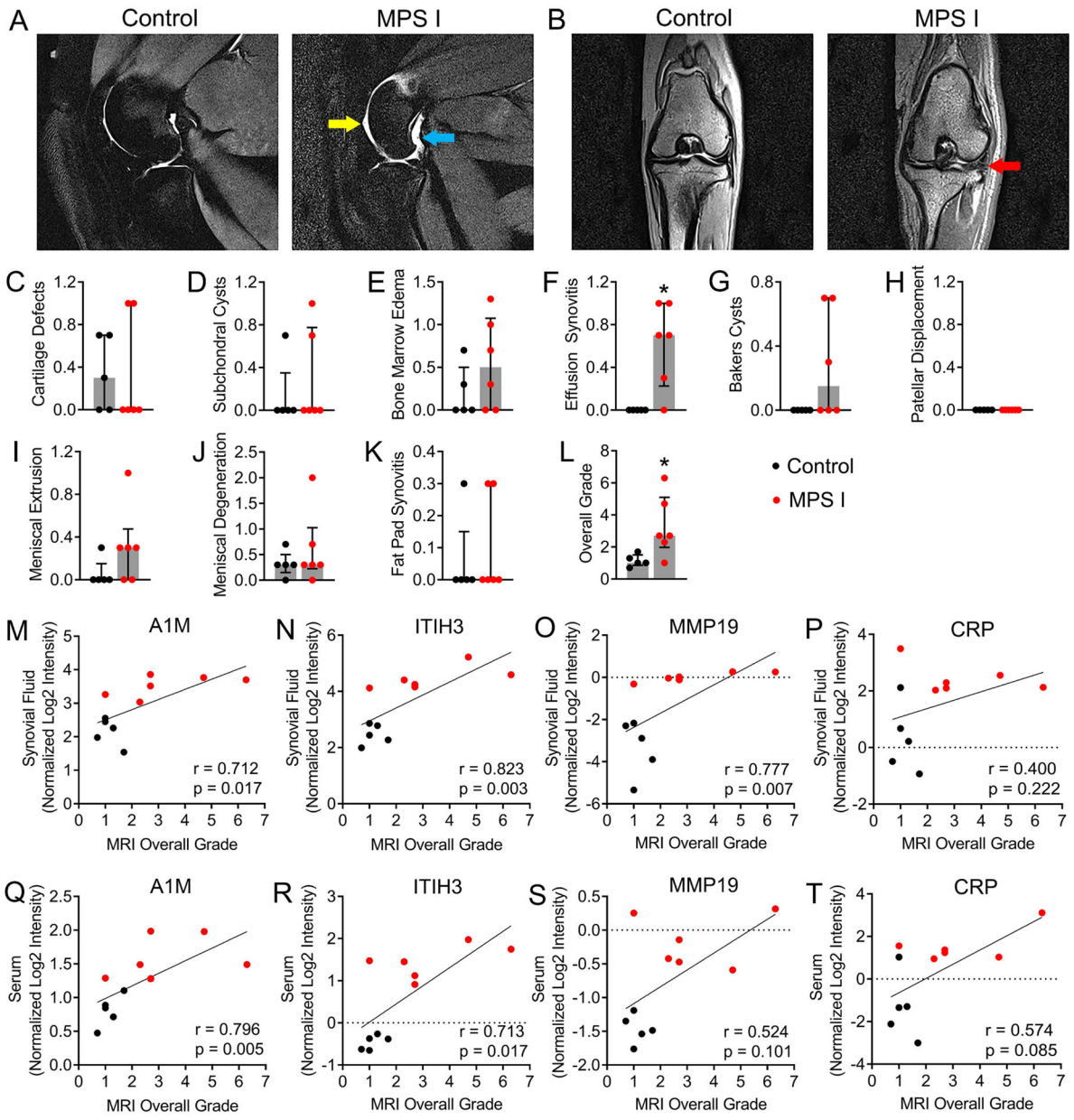

Figure 5.

Magnetic resonance imaging (MRI) of stifle joints from 12-month-old control and MPS I dogs. **A.** Representative T2-weighted, mid-sagittal images showing fluid effusions cranial (yellow arrow) and caudal (teal arrow) to the joint in an MPS I dog. **B.** Representative proton density-weighted, dorsal plane images showing meniscal intrasubstance degeneration (red arrow) in an MPS I dog. **C-L.** Semi-quantitative MRI grades. *p<0.05 vs control; median and interquartile range; Mann-Whitney Test; N = 5–6. **M-P.** Spearman correlations between protein abundance (normalized log2 intensity) in synovial fluid and overall MRI grade. **Q-T.** Spearman correlations between protein abundance (normalized log2 intensity) in serum and overall MRI grade.

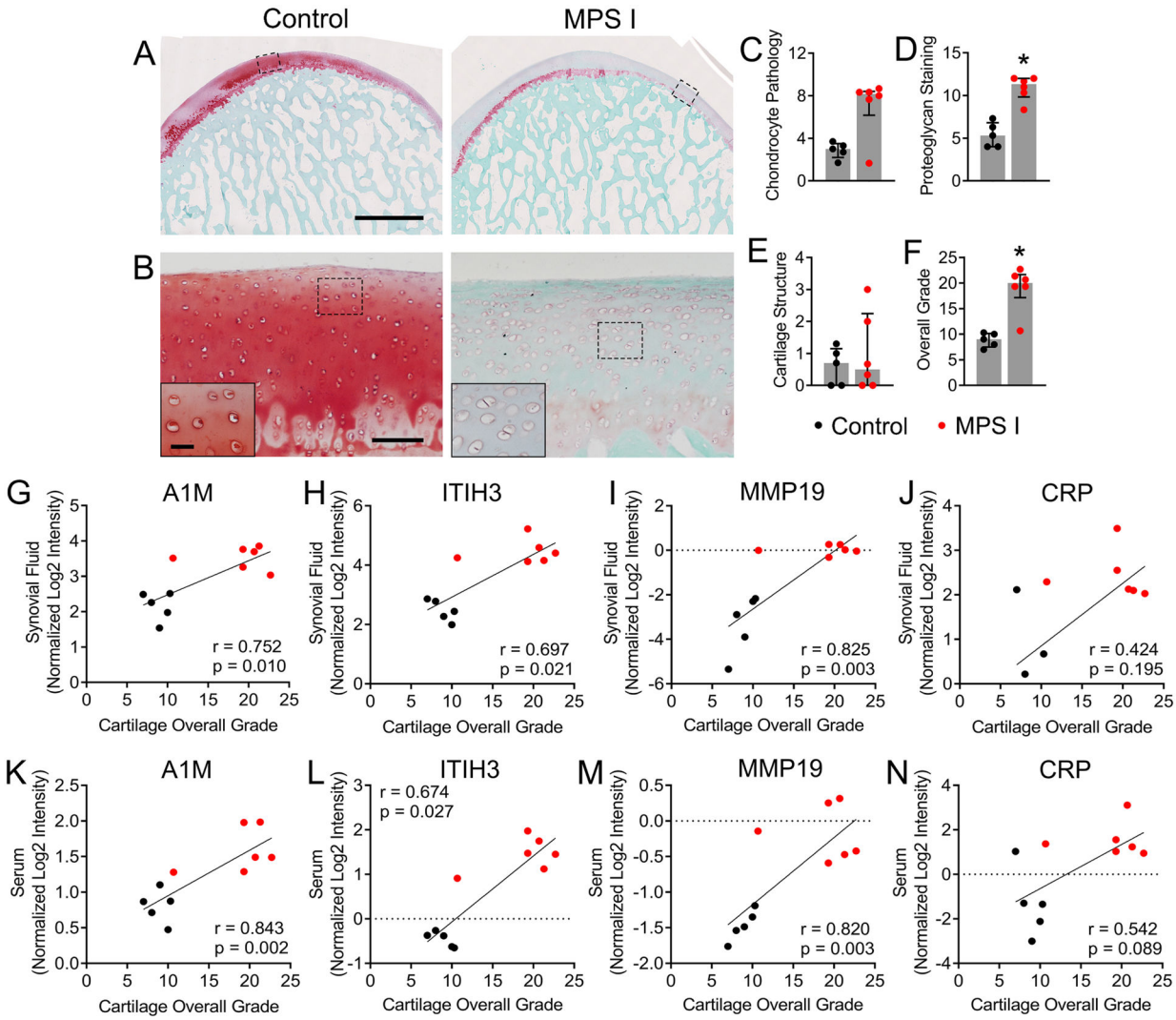

Figure 6.

Histological assessment of femoral condylar cartilage. **A.** Representative mid-sagittal sections of femoral medial condylar cartilage from control and MPS I animals at 12 months-ofage. Scale = 2 mm; Safranin O/fast green staining. **B.** Higher magnification views of the regions indicated in A. showing cell clustering, enlargement and increased density in MPS I cartilage. Scale = 100 μm (inset 30 μm). Quantification of: **C.** Chondrocyte pathology; **D.** Proteoglycan staining; **E.** Cartilage structure; and **F.** Overall cartilage grade. *p<0.05 vs control; median and interquartile range; Mann-Whitney Test; N = 5–6. **G-J.** Spearman correlations between protein abundance (normalized log2 intensity) in synovial fluid and overall cartilage grade. **K-N.** Spearman correlations between protein abundance (normalized log2 intensity) in serum and overall cartilage grade.

Table 1.

Molecules that exhibited significant correlation in abundance between synovial fluid and serum

Symbol	Full Name	Synovial Fluid log2FC	Serum log2FC	Pearson Correlation r value	Pearson Correlation p value
A1M	Alpha-1-microglobulin	1.36	0.78	0.82	0.002
AMY	Alpha-amylase	1.22	1.05	0.85	0.001
ANGPTL 3	Angiopoietin like 3	1.21	0.60	0.82	0.002
AOC3	Amine Oxidase Copper Containing 3	−1.02	−1.36	0.87	0.001
APBB1	Amyloid Beta Precursor Protein Binding Family B Member 1	1.15	0.78	0.80	0.003
APOH	Beta-2-glycoprotein 1	0.63	0.38	0.70	0.016
ATRN	Attractin	0.73	0.66	0.75	0.008
AZGP1	Alpha-2-glycoprotein 1, zinc-binding	1.14	0.99	0.86	0.001
B2M	Beta-2-microglobulin	0.93	1.01	0.69	0.020
C2	Complement C2	0.86	0.53	0.81	0.002
C4A	C4a anaphylatoxin	0.97	0.64	0.86	0.001
C9	Complement C9	0.79	0.84	0.73	0.011
CANT1	Calcium Activated Nucleotidase 1	0.83	1.50	0.80	0.003
CD86	CD86 molecule	1.56	1.59	0.72	0.012
CDH1	Cadherin 1-like	2.22	1.75	0.96	<0.001
CPN1	Carboxypeptidase N subunit 1	1.23	0.98	0.86	0.001
CPN2	Carboxypeptidase N subunit 2	1.04	1.00	0.91	<0.001
CREB3L 3	cAMP responsive element binding protein 3 like 3	2.29	2.26	0.87	0.005
CRP	C-reactive protein	2.12	2.89	0.90	<0.001
EIF4A2	Eukaryotic Translation Initiation Factor 4A2	−1.16	−1.08	0.77	0.006
GANAB	Glucosidase II alpha subunit	0.75	1.97	0.64	0.033
ITIH2	Inter-alpha-trypsin inhibitor heavy chain 2	0.62	0.46	0.75	0.008
ITIH3	Inter-alpha-trypsin inhibitor heavy chain 3	1.99	1.91	0.97	<0.001
LAMP2	Lysosomal Associated Membrane Protein 2	2.37	0.98	0.65	0.029
LBP	Lipopolysaccharide-binding protein	1.21	1.14	0.90	<0.001
LRG1	Leucine rich alpha-2-glycoprotein 1	0.80	0.71	0.74	0.009
MAN2B 1	Alpha-mannosidase	1.84	1.67	0.94	<0.001
MGAM	Maltase-glucoamylase	−0.84	−1.07	0.88	<0.001
MMP19	Matrix metalloproteinase 19	3.35	1.29	0.88	<0.001
ORM1	Orosomucoid	1.47	1.21	0.88	<0.001
PSAP	Prosaposin	1.45	1.35	0.94	<0.001
PTPRG	Protein-tyrosine-phosphatase Receptor Type G	0.81	0.70	0.77	0.006
QSOX1	Quiescin Sulfhydryl Oxidase 1	1.09	0.96	0.90	<0.001
RARRES 2	Chemerin	1.50	1.23	0.82	0.002
SERPIN A3	SERPIN domain-containing protein	0.71	0.34	0.61	0.045
SERPIN A7	Serpin family A member 7	0.71	1.04	0.94	<0.001

Symbol	Full Name	Synovial Fluid log2FC	Serum log2FC	Pearson Correlation r value	Pearson Correlation p value
SPP2	Secreted phosphoprotein 2	1.62	1.23	0.83	0.002
TFRC	Transferrin receptor protein 1	−0.74	−0.91	0.84	0.001
URAH	5-hydroxyisourate hydrolase	1.68	1.48	0.98	<0.001
VSIG4	V-set and immunoglobulin domain containing 4	1.76	1.77	0.70	0.017